Ion exchange and adsorption of cadmium from aqueous media in sodium-modified expanded vermiculite

Henrique Santana de Carvalho Neves[1] · Thiago Lopes da Silva[1] · Meuris Gurgel Carlos da Silva[1] · Reginaldo Guirardello[1] · Melissa Gurgel Adeodato Vieira[1]

Abstract

The use of mineral clays as alternative adsorbent has received attention due to their physicochemical characteristics, superficial negative charge, abundance of vermiculite (especially in Brazil), low cost, and chemical composition, which allows the material modification to increase the adsorptive capacity. This manuscript evaluated the use of expanded vermiculite (EV) and sodium-modified vermiculite (VNa) in the adsorption and ion exchange of Cd^{2+} ions. The sodification was successfully carried out making the ion exchange capacity greater in the modified clay, confirmed by EDX, cation exchange capacity (CEC), DRX, and FTIR analysis. The CEC was 210 and 233 mEq/100 g for the EV and VNa, respectively, with 97.8% exchangeable ion (Na^+) in the VNa. FTIR spectra showed small variations in the groups related to ion exchange and XRD analysis indicated changes in the distance of the layers with loss of crystallinity after clay modification, which was recovered after cadmium adsorption. The kinetics became faster with an equilibrium time of 10 min for VNa and 45 min for EV. Cd^{2+} removal by vermiculite above 99% was achieved. Pseudo-second order model best described the kinetics, in which the resistance to mass transfer in external film is the limiting step of the process and, once this resistance is overcome, the ion exchange happens quickly. Despite the decrease in surface area after sodification, the adsorptive capacity increased 158% in the sodified adsorbent, from 0.107 mmol/g for EV to 0.276 mmol/g for VNa, under the evaluated conditions.

Introduction

The presence of toxic metals in aquatic environments is not a new issue, but it is still of major concern. Although of natural occurrence, anthropic activity is responsible for the release of dangerous levels of them in the environment. This presence creates serious problems for living beings and for the environment as a whole. The toxicity of metals is related to their non-biodegradability and accumulation in the food chain, reaching all trophic levels of the ecosystem (Vardhan et al. 2019; Freitas et al. 2017a).

Cadmium is considered a non-essential metal whose increased concentration in water, soil, and air is related to industrial activities such as non-ferrous mining, batteries, metal finishing, electroplating, textiles, and pigments. Even at low concentrations, cadmium can cause damage to living beings and the aquatic environment. This metal is introduced in the human body by daily food and tobacco smoking, being bound to metallothioneins, accumulating mainly in kidneys and liver. This deposition causes disorders to these organs, such as kidney dysfunction and bone and blood degeneration. Besides, it is carcinogenic (Vardhan et al. 2019), associated with higher risks of coronary heart and cardiovascular diseases and stroke (Chowdhury et al. 2018).

In order to minimize the disposal of hazardous waste present in industrial wastewater in aquatic systems, treatment techniques are currently being studied and employed

---

Responsible Editor: Tito Roberto Cadaval Jr

HSC Neves and TL Silva equally contributed to this work as first authors

✉ Thiago Lopes da Silva
   thiago.lopes.net@gmail.com

[1] Department of Processes and Products Design, School of Chemical Engineering, University of Campinas, Albert Einstein Avenue, 500, Campinas, São Paulo 13083-852, Brazil

to remove contaminants, as dissolved metals from industrial effluents. Among the proposed processes, adsorption is a promising one due to the simplicity and flexibility of operation, the possibility of using industrial waste and alternative materials as an adsorbent, and the possibility of removing a wide range of pollutants (Silva et al. 2016; Volesky et al. 2001). Among alternative adsorbents, mineral clays attract attention due to their physicochemical characteristics, quantity, and low cost for contaminants remediation (Sarkar et al. 2019). The use of clays for contaminant adsorption include the use of Verde-lodo bentonite for caffeine (Oliveira et al. 2019), and silver and copper ions (Freitas et al. 2017b), bentonite and modified bentonite for silver (Cantuaria et al. 2014, 2015, 2016), nickel and copper ions (Almeida Neto et al. 2014) and multi-metals (Pb^{2+}, Cd^{2+}, and Mn^{2+}) (Alexander et al. 2017), organoclay for benzene, toluene, and xylene (BTX) (Lima et al. 2017), vermiculite with polyaniline for Cr^{4+}, Mo^{4+}, W^{4+}, V^{5+}, and P^{5+} (Ryabchenko et al. 2014), and expanded vermiculite for zinc ions (Nishikawa et al. 2012), for binary zinc and copper ions (Freitas et al. 2017a), and neodymium (Brião et al. 2020), among others.

Vermiculite comes from igneous rocks and is found mainly in mountainous lands (Potter 2010). Brazil stands out in the world as one of the largest producers of vermiculite for commercial purposes (US Geological Survey, Mineral Commodity Summaries 2021). Vermiculite clay is a phyllosilicate mineral whose structural configuration is based on layers. It is classified as type 2:1, consisting of an octahedral layer between two tetrahedral sheets (Howard and Lekse, 2018). The tetrahedral layer consists of SiO_4 and the octahedral layer is composed of $Mg(OH)_2$ and $Al(OH)_3$ (Freitas et al. 2017a). Aluminum (Al^{3+}) and iron (Fe^{3+}) cations are often found in the tetrahedral sheets of the clay structure. In the octahedral layers, it is common to find iron (Fe^{2+} and Fe^{3+}) and magnesium (Mg^{2+}) cations, and manganese (Mn^{2+}), nickel (Ni^{2+}), lithium (Li^+), zinc (Zn^{2+}), copper (Cu^{2+}), and chromium (Cr^{3+}) are less frequent. The presence of cations in interlamellar spaces allows ionic exchange with cations in the solution, which is an important property in the performance of the clay as an adsorbent. In addition, the mineral's surface is negatively charged and hydrophilic, which makes it an excellent adsorbent for cationic and hydrophilic pollutants (Sharkar et al. 2019; Howard and Lekse 2018; Freitas et al. 2017a). When heated until high temperatures in a short period of time, the water present in the vermiculite structure can be quickly evaporated, promoting a disruptive effect on the solid structure, increasing the distance between its layers by the process called exfoliation. As a result, the expanded vermiculite is produced with characteristics of greater porosity and larger surface area (Marcos and Rodríguez 2014).

The aim of this study was to evaluate the removal of Cd^{2+} ions by adsorption and ion exchange processes in expanded vermiculite and sodium-modified vermiculite (sodified vermiculite). The adsorptive and ionic exchange kinetic behavior was evaluated with the use of mathematical models to elucidate the mechanisms involved. Both clays were characterized before and after adsorption. The chemical composition of the surface, the surface load as a function of pH and the zeta potential of the solid, the surface area, pore volumes, ion exchange capacity, solid morphology, and the study of metallic speciation were also performed.

Methods

Materials

The reagents used for the preparation of the solutions and pH control during the experiments were cadmium nitrate ($Cd(NO_3)_2.4H_2O$, 103,7%, Vetec, Brazil), nitric acid (HNO_3, 65,88%, Anidrol), and ammonium hydroxide (NH_4OH, Dinâmica, Brazil). All reagents were standard analytical. The solutions used in the experiments were prepared with acidified water at pH 6, according to the pH evaluation carried out in this study. The Brazilian vermiculite clay was kindly donated by Brasil Minérios Company (Goiás, Brazil).

Adsorbents' preparation

The expanded vermiculite clay (EV) and the modified clay by the sodification process (VNa) were evaluated. The clays obtained after the adsorptive process were designated by EV-Cd and VNa-Cd, indicating that the material was contaminated with cadmium metallic ions.

For the experiments, the EV was rinsed with 4 L of deionized water, dried for 24 h, at 105 °C, and sieved to obtain an average diameter of 0.855 mm. In the rinsing process, the clay particles were placed on filter paper and deionized water was slowly poured over them to promote the solid washing. For VNa preparation, EV was treated with sodium in an acid medium. EV was placed in contact with a 1% NaCl solution at pH 3 (pH adjusted with 0.1 mol/L HNO_3 solution) in the proportion of 10:1 (g:L), under agitation (120 rpm) for 3 h as described by Almeida Neto et al. (2014). After that, the clay was washed with 4 L of deionized water in a filter paper. At the end of the process, the filtrate sodium concentration was zero, indicating that all sodium not adhered to the solid was removed from the adsorbent surface. The material obtained was dried (105 ºC, 24 h) and sieved (0.885 mm). This procedure was performed twice, making the material ready for its use as an adsorbent.

Cadmium removal kinetics

The kinetic tests were performed using 1500 mL of metallic ion solution at concentrations of 0.5, 1, and 2 mmol/L and 15 g of adsorbent (adsorbent dosage: 10 g/L). The mixture was kept under constant magnetic stirring, at room temperature (25 °C), and the pH was carefully controlled at 6 to avoid chemical precipitation. At pre-set times, 4-mL samples were collected, centrifuged, and filtered (0.45 μm syringe filter, Millipore). The metal liquid phase concentrations, Cd^{2+} and the exchangeable ions (Ca^{2+}, Na^+, Mg^{2+}, and K^+), were determined by atomic absorption spectrophotometry (AA-7000, Shimadzu, Japan). The amount adsorbed (q) was determined by Eq. (1).

$$q = \frac{(C_0 - C_t).V}{m} \tag{1}$$

where C_0 is the initial metal concentration, C_t is the concentration at time t (mmol/L), V is the volume of metal solution (L), and m is the adsorbent mass (g).

The pseudo-first order (PFO) (Lagergren 1898), pseudo-second order (PSO) (Ho and Mckay 1998), intraparticle diffusion (ID) (Weber and Morris 1963), Boyd (Boyd et al. 1947), and resistance to mass transfer in the external film (RMT) (Puranik et al. 1999) models were adjusted to the kinetic data using Origin 7.0 and Maple 17 software.

To evaluate the effect of ion exchange, control experiments with vermiculite (EV) and deionized water were performed under the same conditions of the kinetic experiments. The concentrations of Ca^{2+}, Na^+, Mg^{2+}, and K^+ were determined in liquid phase of control experiments, and the values were subtracted from those determined in kinetics, to assess the behavior of ion exchange.

Cation exchange capacity (CEC) and amount of exchangeable ions

The cation exchange capacity (CEC) is the ability of a material to exchange and retain positively charged ions on its surface. The exchangeable ions amount consists in separately determining the concentration of exchangeable Ca^{2+}, Na^+, Mg^{2+}, and K^+ ions present in the adsorbent structure. The CEC was determined in triplicate, according to Almeida Neto et al. (2014), in which the exchangeable ions of EV and VNa are displaced by NH_4^+ ions into a liquid phase. Each ion concentration was determined by atomic absorption spectrophotometry.

For exchangeable ions displacement, 1 g of washed and dried EV clay was stirred in 20 mL of 3 mol/L ammonium acetate solution at pH 7 for 24 h. Subsequently, the supernatant was centrifuged and filtered (0.45 μm syringe filter, Millipore) for the exchangeable ion concentration determination.

The exchangeable light metals concentration in solid phase and the CEC were calculated by Eqs. (2) and (3), respectively.

$$q_{LM} = C_{LM}.\frac{V_{NH_4^+}}{m} \tag{2}$$

$$CEC = \frac{\sum (z_{LM}.C_{LM}).V_{NH_4^+}.100}{m} \tag{3}$$

where CEC is the cation exchange capacity (mEq/(100 g of clay)), q_{LM} is the light metal concentration in solid phase (mmol/g), C_{LM} is the light metal concentration in solution (mmol/L), $V_{NH_4^+}$ is the volume of 3 mol/L ammonium acetate solution (L), m is the solid sample mass (g), z_{LM} is the exchangeable light metal charge.

Metal speciation

The metal speciation diagrams as a function of pH were simulated by Hydra software that uses the Medusa thermodynamic database (Puigdomenech 2010). From these diagrams, it is possible to estimate the pH at which value of the chemical precipitation of the metal species present in the liquid phase occurs.

Adsorbents' characterization

The adsorbents' characterization was performed before and after the Cd^{2+} ion adsorption. The morphological structure and the semi-quantitative chemical composition were evaluated by SEM–EDX technique: scanning electron microscopy coupled with energy dispersive X-ray (LEO Electron Microscopy, LEO 440i/6070—England) with magnification of 150 and 2500× (10 kV, 50 pA). The identification of the clay functional groups was performed by Fourier transform infrared spectroscopy (FTIR), in the range 4000–400 cm^{-1} using KBr pellets (Thermo Scientific, Nicolet 6700—Madison, USA). The zeta potential and the surface charge as a function of pH determination were carried out in the SurPASS Electrokinetic Analyzer (Anton Paar, Austria) equipment. The electrolyte solution was ammonium acetate (CH_3COONH_4; 1 mmol/L) and the acidic and basic titrating solutions were nitric acid (HNO_3, 0.1 and 0.5 mol/L) and ammonium hydroxide (NH_4OH, 0.4 mol/L) solutions.

The surface area was determined by N_2 physisorption (BET) (Quantachrome/NOVA1200e, Germany) at 77 K. The N_2 adsorption and desorption isotherms could be used to estimate the volume of micropores (V_{mic}) and mesopores (V_{mes}) by the BJH method (Barrett-Joyner-Halenda). These values could be estimated using Eqs. (4) and (5) (Gañán-Gómez et al. 2006).

$$V_{mic} = V_{ads(P/P_0=0.10)} \tag{4}$$

$$V_{mes} = V_{ads(P/P_0=0.99)} - V_{ads(P/P_0=0.10)} \tag{5}$$

where V_{ads} is the volume adsorbed up to the relative pressure (P/P_0).

Statistical treatment for the model adjustments

For the statistical analysis of the models' adjustments to the experimental data, the evaluated parameters were the determination coefficient (R^2) (Eq. (6)), the relative mean deviation (Eq. (7)), and the corrected Akaike criterion (AICc) (Eq. (8)) (Bonate 2011).

$$R^2 = \frac{\sum_{i=1}^{N}(q_{i,calc} - \overline{q_{exp}})^2}{\sum_{i=1}^{N}(q_{i,exp} - \overline{q_{exp}})^2} \tag{6}$$

$$RMD = \frac{\sum_{i=1}^{N}\left|\frac{q_{i,calc}-q_{i,exp}}{q_{i,exp}}\right|}{N} \tag{7}$$

$$AIC_c = N.ln\left(\sum_{i=1}^{N}\frac{(q_{i,exp} - q_{i,calc})^2}{N}\right) + 2p + \frac{2p(p+1)}{N-p-1} \tag{8}$$

where $q_{i,calc}$ is the adsorption capacity calculated by the proposed model at point i (mmol/g), $q_{i,exp}$ is the experimental adsorption capacity at point i (mmol/g), $\overline{q_{exp}}$ is the adsorption capacities average (mmol/g), N is the total number of points collected in the same experiment, and p is the adjustable parameter number in the proposed model.

The AICc parameter was applied because it shows greater sensitivity in detecting the best model in samples with a small number of points ($N/p < 40$). Lower AICc values indicate better adjusting among other tested models (Bonate 2011).

Results and discussion

Characterization before and after adsorptive process

The characterization analyses were carried out on the clays before (EV and VNa) and after (EV-Cd and VNa-Cd) the adsorptive process to evaluate the changes that the

sodification and cadmium adsorption processes promoted in the adsorbents.

The atomic percentage of the constituent elements of the surface clays were determined by semi-quantitative EDX analysis and are shown in Table 1. Due to this semi-quantitative analysis character, the values represent an average of 5 measures. This analysis was used to support the determination of exchangeable ions and the effectiveness of the ion exchange.

In general, vermiculites have in their composition a high amount of Mg, which classifies the materials as a magnesian clay mineral. The expanded vermiculite sodification to produce VNa changes the clay constituents' percentages. The sodium addition process in acid medium promoted the removal of K and Cr and changes in the percentages of Fe, Mg, Ti, Al, and Si in the VNa composition. Probably, these atoms were leached out in the acid medium and replaced by Na, as observed in the increased percentage of the latter element in VNa compared to EV, indicating that the sodium treatment was effectively carried out. As expected, after the adsorptive process, it is observed that cadmium is present in both contaminated clays (EV-Cd and VNa-Cd). It was found out that Na is still present in the contaminated VNa-Cd clay composition, revealing that not all the sodium added in the solid in the sodification was replaced by cadmium after adsorption. However, this fact may be related to the small amount of cadmium in solution at the end of the adsorptive process because removals greater than 99% were obtained in all performed experiments (discussed details further in Fig. 8).

The EV, EV-Cd, VNa, and VNa-Cd adsorbent morphologies were investigated by scanning electron microscopy (SEM) with of 150×, 400×, and 2500× magnifications, as shown in Fig. 1.

In the micrographs, the vermiculite lamellar structure can be clearly seen. The EV clay shows a large gap between the lamellae indicating a high degree of the expanded vermiculite exfoliation. In comparison, in the contaminated with Cd^{2+} expanded vermiculite (EV-Cd), a smaller distance between the lamellae is observed and, more markedly, smaller distances were also seen in the modified (VNa) and in the contaminated clays (VNa-Cd). After the treatment with sodium and the Cd uptake, the particle becomes more compacted. The observed retraction occurs due to water absorption in various steps that the clays are subjected.

Table 1 Atomic percentage of the elements detected by EDX for the expanded and sodified vermiculite samples, before and after contamination with Cd^{2+}

	Mg	Al	Si	K	Ti	Cr	Fe	Na	Cd
V	32.3	13.5	40.2	8.0	1.0	0.4	4.5	0	0
VNa	35.9	12.7	41.2	0	0.2	0	2.7	7.1	0
EV-Cd	38.3	14.7	41.6	0	0.4	0	2.5	0	2.4
VNa-Cd	45.6	6.5	44.5	0	0.3	0	1.3	0.5	1.3
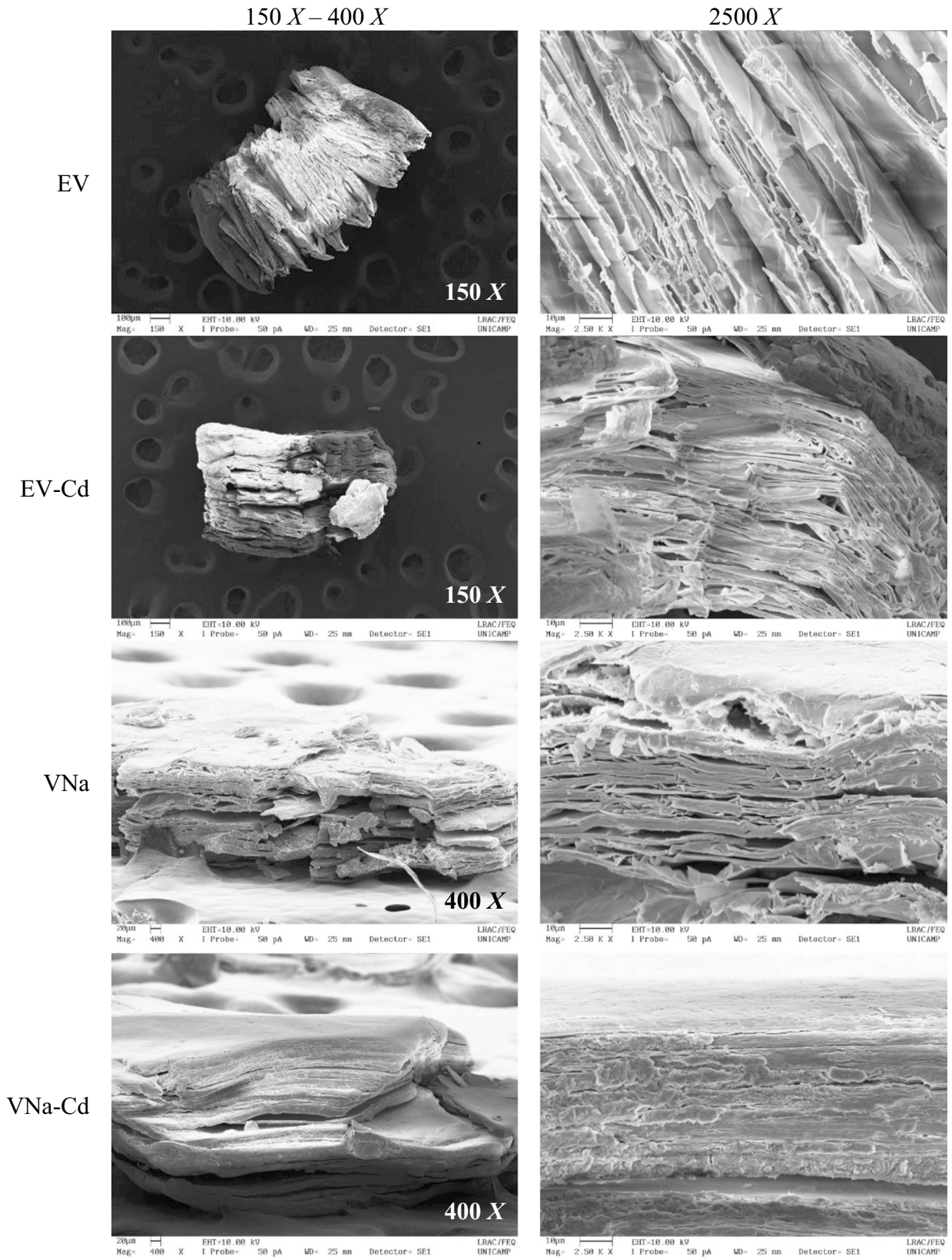
Fig. 1 EV, EV-Cd, VNa, and VNa-Cd clay micrographs with 150×, 400×, and 1500×magnification

The EV-Cd clay was put in contact with water during the adsorption process, the VNa clay was placed in contact with an aqueous medium in the sodification process, and finally the VNa-Cd clay had contact with water twice (in the sodification and adsorption processes). Similar results were observed by Stawinski et al. (2017) in particle morphology after combined acid–base treatment of vermiculite and expanded vermiculite. The authors reported a decrease in basal spacing, particle size, and platelet fragmentation occurrence after treatment. Nishikawa et al. (2012) also observed decreases in spacing between the lamellae and superficial roughness of the expanded vermiculite after the zinc ion adsorption.

From Fig. 1, smaller surface areas are expected in the contaminated clays and especially in the contaminated modified clay (VNa-Cd), which was confirmed by the specific surface area analyses. Table 2 displays the results of surface area and micropore and mesopore volumes, and Fig. 2 depicts the adsorption and desorption isotherms of N_2 (BET).

From Table 2, reductions in surface areas and clays' micro- and mesopore volumes are observed after adsorption and treatment with sodium, in comparison with EV clay. The decrease in these values is due to the lamellae contraction, which can be observed in the SEM micrographs (Fig. 1).
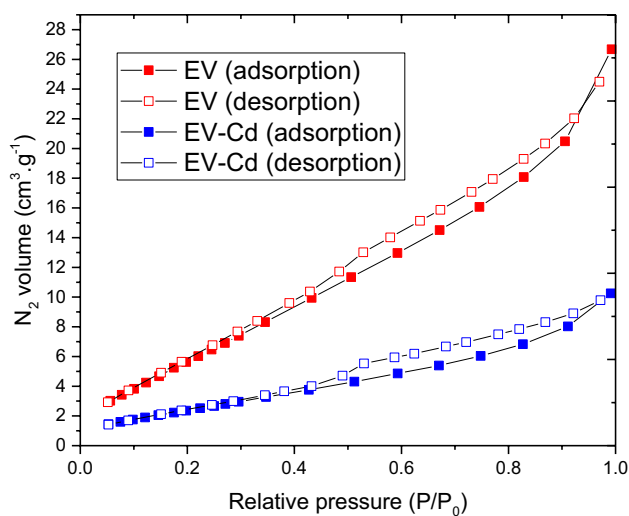
The isotherms of Fig. 2 (A) and (B) indicate that both showed similar behavior, with a more pronounced hysteresis for sodified vermiculite. Hysteresis occurs when the pore width exceeds a critical value, favoring capillary gas condensation. According to the classification standards proposed by IUPAC, these isotherms are closer to type IV(a), common to mesoporous adsorbents. Regarding the observed hysteresis in all isotherms, both are similar to type H3, which occurs in non-rigid aggregate materials formed by lamellae, as it is the case of vermiculite (Thommes et al. 2015).

The identification of functional groups in the EV, EV-Cd, VNa, and VNa-Cd particles was determined by FTIR analysis, and all spectra obtained are shown in Fig. 3.
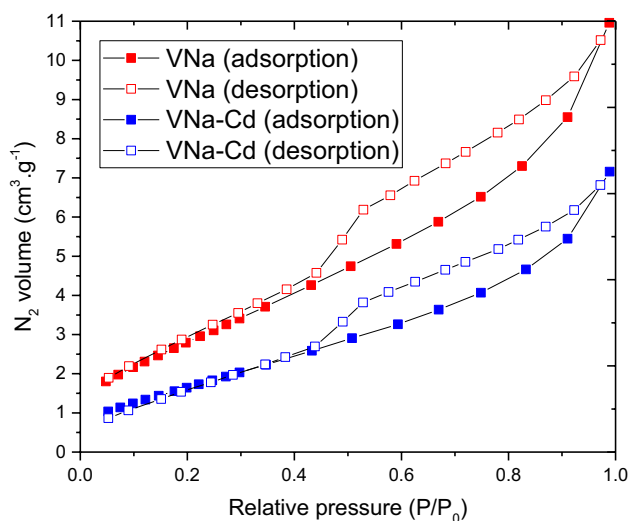
The FTIR spectra are characteristic of trioctahedral phyllosilicates such as vermiculite (Russell and Fraser 1994). The peaks in the ranges 3411–3483 cm^{-1} and 1631–1644 cm^{-1} are observed due to the stretching and bending vibration of the O–H of water molecule adsorbed by hydrogen bonds (Moraes et al. 2019; Lima et al. 2019; Marcos and

Fig. 2 Adsorption and desorption isotherms of N_2 in (A) expanded vermiculite before (EV) and after (EV-Cd), and in (B) sodified vermiculite before (VNa) and after (VNa-Cd) contamination with Cd^{2+}

Rodríguez 2014). Other ranges are observed between 1002 to 1004 cm^{-1} that occur because of Si–O–Si and Si–O–Al stretching bond vibrations, 665 to 673 cm^{-1} that is related to bending vibration of Si–O, and 441 to 459 cm^{-1} which is attributed to bending of Si–O–R vibrations (considering R metals like Mg, Al, Fe, and Si) (Marcos and Rodríguez 2014). In this last band, variations were observed between the clays before and after the adsorptive process. The peaks varied from 459 to 447 cm^{-1} (to EV and EV-Cd) and from 454 to 442 cm^{-1} (to VNa and VNa-Cd), indicating that this is a possible site of ion exchange in both adsorption and sodification. In addition, the observed 1384 cm^{-1} peak after cadmium adsorption (to EV-Cd and VNa-Cd) refers to OH bending and Si–O stretching and bending absorptions
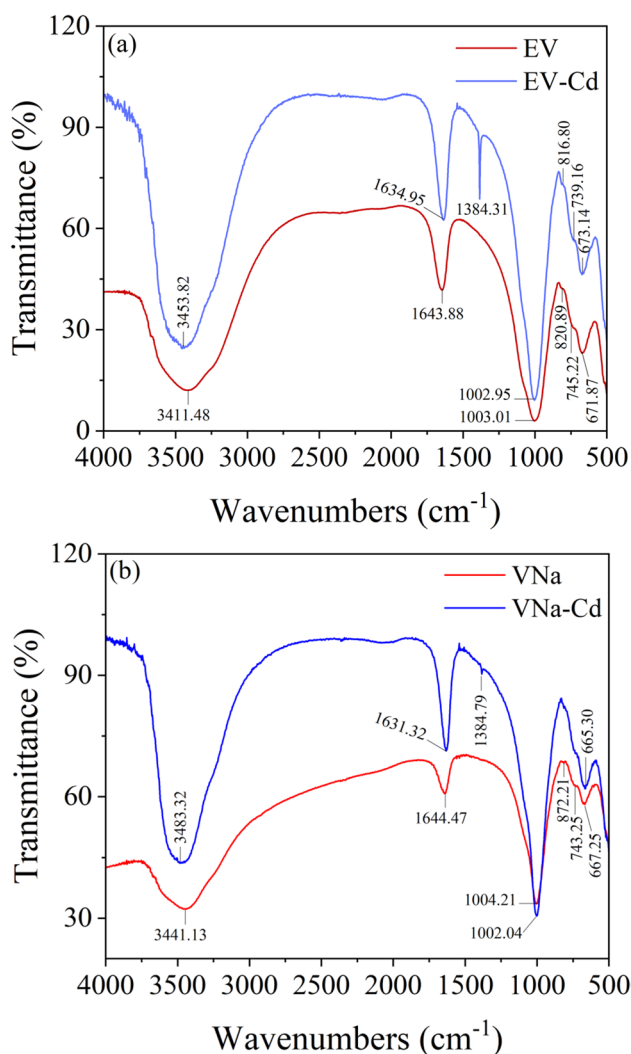
Table 2 Surface area and micro- and mesoporous volumes of adsorbents before and after Cd adsorption

	EV	EV-Cd	VNa	VNa-Cd
Surface area (m^2/g)	26.518	9.889	11.084	6.700
Micropores volume (cm^3/g)	3.828	1.765	2.176	1.250
Mesopores volume (cm^3/g)	22.638	8.469	8.783	5.908

Fig. 3 FTIR spectra of VE, VNa, VE-Cd, and VNa-Cd

(Madejová 2003). Since the sodification process involves the displacement of clay metals by sodium, which is later replaced by cadmium after adsorption, changes in the spectrum related to Si–O–R bonds can be observed. This fact is also in accordance with the EDX analysis presented in Table 1, which demonstrates the modification of clay constituents in EV, EV-Cd, VNa, and VNa-Cd. Despite this assertion, an overview shows little variation among all spectra, that is, both sodium treatment and adsorption (contamination) did not affect the structure of vermiculite significantly. This behavior is in agreement with other literature results. Moraes et al. (2019) performed a sodification procedure different from the one used in the present work and, even so, no pronounced modification was observed in the spectra of the adsorbents. Basically, the exchangeable light metals in vermiculite (Mg^{2+} and Na^+) remain physically bound at the vermiculite surface, and thus are easily exchanged for Na^+ ions. The small variation observed in the curves and the difficulty

in identifying variations by IR spectroscopy occur because there are no characteristic absorption bands (or sharp peaks) in the vermiculite that are easily recognized in the complex matrix of the mineral (Russell and Fraser 1994).

Figure 4 shows the X-ray diffraction patterns for the samples before and after the adsorptive process. EV and VNa showed characteristic peaks of the interlayer distance of vermiculite (referring to the region between 1.4 and 1.5 nm), representative of two water layer hydration state (Moraes et al. 2019). Furthermore, Fig. 4b (VNa) indicated the presence of two phases due to a peak around 1.5 nm, related to the Mg^{2+}-vermiculite, and another peak of higher intensity at 1.2 nm, referring to Na^+-vermiculite. Thus, although the treatment did not completely modify the adsorbent, the analysis indicates a greater presence of the phase formed by the complex with sodium (Pérez-Maqueda et al. 2003). The sodification process of the EV leading to the VNa formation decreases the structural organization of the solid, inducing decreases in the reflections intensity and clay crystallinity in its sodified form (VNa). This fact probably occurs due to the insertion of the hydrated ion of the alkali metal that causes an enlargement in the clay interlayer space, which can be observed by the increase of the basal space of EV and VNa: 1.42 and 1.45 nm, respectively Lima et al. 2019; Moraes et al. 2019; Anjos et al. 2014). The observed changes confirm that the sodification process was successfully carried out by leaching and ion exchange of the ions present in the region between layers. In this case, previously, there were predominantly divalent ions (Mg^{2+}) that were replaced by monovalent ions (Na^+). Similar XDR patterns were obtained in works that aimed the investigation of vermiculite and modified vermiculite (Lima et al. 2019; Moraes et al. 2019 and Anjos et al. 2014). After sample contamination by cadmium (Fig. 4 (C) and (D)), both EV-Cd and VNa-Cd showed interlayer distance in the characteristic region of vermiculite. In addition, the EV-Cd and VNa-Cd diffractograms have a similar pattern to that of expanded vermiculite, indicating that the replacement of the exchangeable ions by Cd^{2+} (that have the same valence of Mg^{2+}) promotes a crystalline structure close to that of Mg-vermiculite, that is, the cadmium adsorption recovered the crystallinity lost in the VNa preparation.

pH evaluation and selection

The pH used in the adsorptive experiments was defined from the metal speciation simulation and surface charge analysis. The obtained diagrams for the initial cadmium ion concentrations of 1.0, 1.5, and 2.0 mmol/L are presented in Fig. 5.

From the diagrams (Fig. 5), it is observed that for all concentration values, the cadmium precipitation to hydroxides species occurs at a pH greater than 8. At pH < 8, only the ionic form of Cd^{2+} is present in the solution. Thus, at pH < 8,

Fig. 4 XRD patterns of EV, VNa, EV-Cd, and VNa-Cd clays
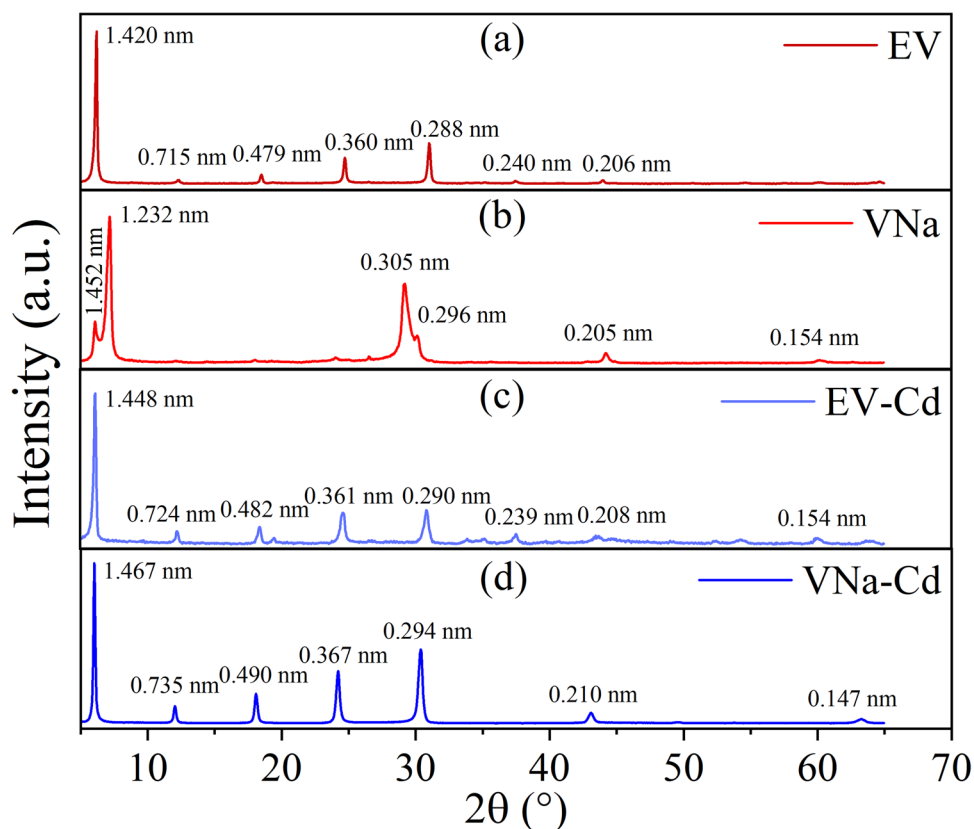
any variation in the metal concentration can be related only to metal adsorption and ion exchange between the metal in solution and the adsorbent solid constituents. The surface load as a function of pH and zero load potential (isoelectric point pH_{ZPC}) of EV and VNa clays are shown in Fig. 6.

The pH_{ZPC} close to 2.5 was observed for VE. At pH above the pHzpc value, the solid surface becomes negatively charged. For VNa, the charge is negative throughout the pH range studied, with values below those observed for EV. Liu et al. (2017) observed pH_{ZPC} values equal to 2, and Sis and Uysal (2014) and Chen et al. (2018) observed negative charge values across the pH range for expanded vermiculite and vermiculite respectively. In both cases, the solid surface's negative charge may favor the adsorption of positively charged species by electrostatic forces. The lower values of VNa charge compared to EV indicate that the sodification leads to the release of much of the positive charge of the exchangeable ions on the surface in addition to the new anionic adsorption sites formation. This reduction in surface charge reveals that the treatment favored the vermiculite cation attraction potential.

From the speciation diagrams and surface charge and pH_{ZPC} analysis, the pH selected for adsorption experiments was 6. This value is within the range of 2.5 and 8 and in a region in which the surface charges are stable for EV and VNa. The stability of surface charge values, within an adsorption operating range, is important because small variations in pH can significantly affect the adsorptive process when it comes from electrostatic charges.

## Cation exchange capacity (CEC) determination

The CEC results and the amount of exchangeable ions experiments are displayed in Table 3.

According to Table 3, an increase in cation exchange capacity was observed after the vermiculite treatment with sodium. The determined values for both adsorbents are among the values reported in the literature by Malandrino et al. (2006) of 120 mEq/100 g and Nishikawa et al. (2012) of 445 mEq/100 g for EV. The parameter greatest variation is due to differences in the clay's batch composition.

For the EV, the exchangeable ion composition showed a majority proportion of Mg^{2+}. Small amounts of K^+ and Ca^{2+} ions were also found, representing less than 5% of the total cations. For the VNa, the exchangeable ion Na^+ represented 97.8% of the total, indicating that the selected sodium treatment for this study achieved the desired result. Residual Mg^{2+} ions could be eliminated with a repeated sodium treatment; however, it was not necessary.

The adsorption experiments were carried out at pH 6. pH is an important factor in the ion exchange capacity. At low pH, H^+ ions compete with other cations for exchange on the

Fig. 5 Cadmium ($Cd(NO_3)_2$) metallic speciation in aqueous medium with initial Cd concentrations of 1.0, 1.5, and 2.0 mmol/L
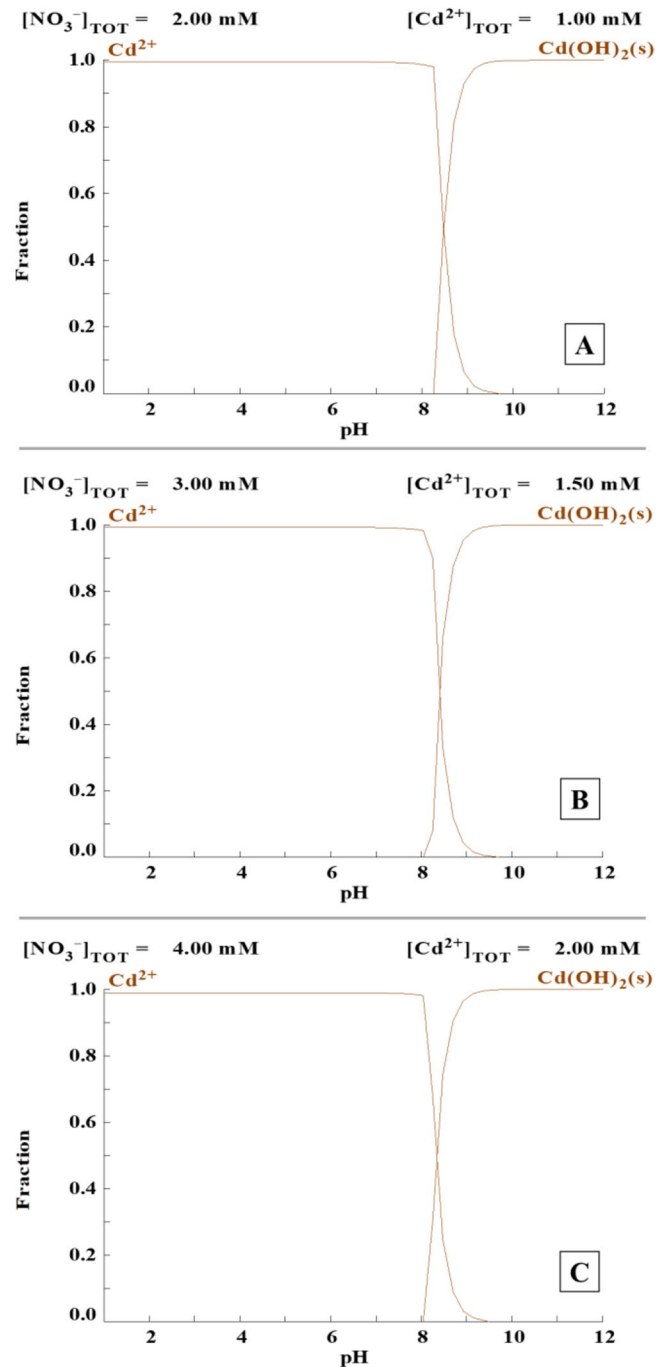

surface adsorbent, and this influence decreases as the pH increases. At pH > 7, the OH^- group begins to neutralize surface charges. At pH 6, cation exchange may be related to a lesser extent to broken bonds and mainly to substitutions within the lattice structure. Bond breakage occurs at the silica-alumina edges, creating charges that are balanced by cations in solution. In the second case, the charges are unbalanced by substitutions of the clay constituent ions that can be replaced by ions of the clay structure itself. However, there will always be a charge deficiency on the surface allowing cations to be adsorbed on the vermiculite layer surfaces (Mathialagan and Viraraghavan 2003).
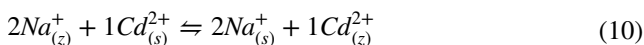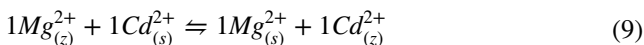
Ion exchange process

During the kinetics study, the relevant light metal profiles were evaluated as a function of time. According to the exchangeable ion quantity analysis, the systems with EV and VNa presented exchangeable ion proportions of 97% Mg^{2+} and 97.8% Na^+, respectively. To simplify the experiments,

Fig. 6 Profiles of the expanded vermiculite (EV) and sodified vermiculite (VNa) zeta potentials

EV clay

VNa clay
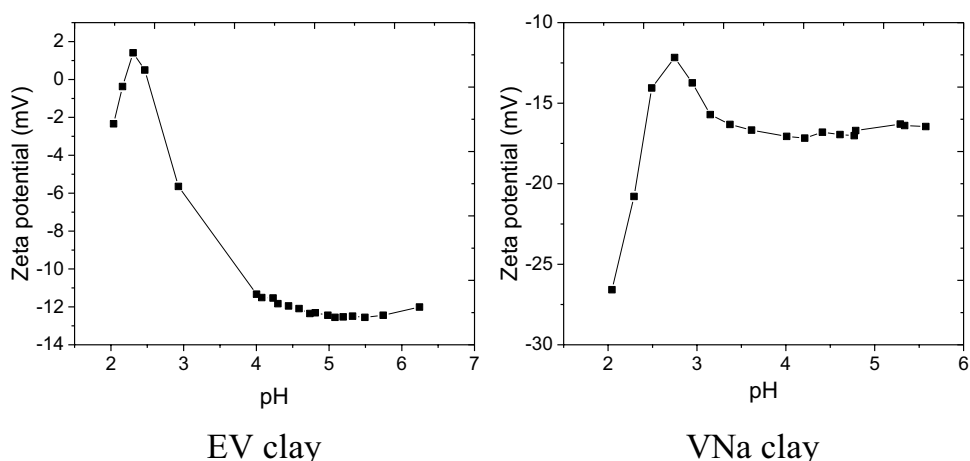
other components, such as K^+ and Ca^{2+}, were considered insignificant in the ion exchange kinetics.

Figure 7 presents the kinetics profiles, control experiments, and theoretical ion exchange profiles for the systems with EV and VNa, obtained for initial concentrations of 1, 1.5, and 2 mmol/L. The concentrations are given in mEq/L, as this unit takes into account the amount of charges involved in the exchange, enabling a direct comparison of the theoretical and experimental profile. The light metal theoretical concentration is calculated considering the amount of exchangeable ion that it would desorb if the ion exchange stoichiometry was satisfied. Theoretical stoichiometric reactions are represented by Eqs. (9) and (10) for the systems with EV and VNa, respectively.

$$1Mg^{2+}_{(z)} + 1Cd^{2+}_{(s)} \leftrightharpoons 1Mg^{2+}_{(s)} + 1Cd^{2+}_{(z)} \tag{9}$$

$$2Na^{+}_{(z)} + 1Cd^{2+}_{(s)} \leftrightharpoons 2Na^{+}_{(s)} + 1Cd^{2+}_{(z)} \tag{10}$$

where the subscripts (z) and (s) indicate that the ions are in the solid phase and in solution, respectively. The theoretical concentration of the released light metal, in mEq/L, can be calculated using Eq. (11).

$$C_{LM(theoretical)} = \frac{z_{Cd}}{z_{LM}}[C_{Cd0} - C_{Cd}(t)] \tag{11}$$

where z is the ion charge, C_{Cd0} (mmol/L) is the initial Cd^{2+} concentration solution, $C_{Cd}(t)$ (mmol/L) is the

concentration of Cd^{2+} at time t, and the subscript LM refers to the light metal.

The profiles observed in both cases show great similarity to that described by Borba et al. (2010), where Cd^{2+} concentration in the fluid phase reduces simultaneously with the increase of the metal initially present in the ion exchange site. The released metal concentration showed an oscillation at the beginning of the equilibrium, probably due to the high affinity for the fluid phase of the light metal, in which the rapid phase change causes the equilibrium concentration to be exceeded.

To assess whether electroneutrality was reasonably satisfied during ion exchange, the released ion percentage, in relation to the theoretical one, was calculated at equilibrium. For the EV tests, 110.7, 97.7, and 92.8% Mg^{2+} were released in relation to the theoretical one, for the kinetics of 1, 1.5, and 2 mmol/L, respectively. As the values oscillated close to 100%, it is reasonable to assume that the reactions were stoichiometric. These deviations are probably related to experiments and measurement error propagation. Therefore, the mechanism that governs the Cd^{2+} removal by this clay is predominantly ion exchange.

In the case of VNa, for the kinetics of 1, 1.5, and 2 mmol/L, 70.2, 70.4, and 75.1% of the expected theoretical Na^+ were released. This suggests that part of the cadmium is removed by another additional adsorptive mechanism. Possibly, the new adsorption site availability is due to the treatment carried out during sodification, in which the sample was submitted to acidic pH. At low pHs, H^+ ions can move

Table 3 Cation exchange capacity (CEC) and each exchangeable metal capacity of EV and VNa

Clay	CEC (mEq/100 g)	q_{Mg}(mmol/g)	q_{Na}(mmol/g)	q_K(mmol/g)	q_{Ca}(mmol/g)
EV	10.44 ± 7.46	1.0216 ± 0.1025	-	0.0181 ± 0.0056	0.0125 ± 0.0029
VNa	33.19 ± 16.9	0.0508 ± 0.0110	2.2711 ± 0.3284	-	-

light metals into the solution, in addition to modifying the clay structure and exposing new pores.

Adsorptive process

The cadmium adsorption kinetics using commercial expanded vermiculite (EV) and sodium-treated vermiculite (VNa) were carried out in 3 different initial concentrations (1.0, 1.5, and 2.0 mmol/L), at 25 °C. The pH was constantly monitored and adjusted to 6 with a nitric acid solution (0.1 mol/L). The plots of adsorbed amount (q) versus time (t), for all initial conditions, are shown in Fig. 8.

From Fig. 8 (a), it can be seen that the kinetic profiles are very close for the 3 initial concentrations. The cadmium-adsorbed amounts by EV in equilibrium (q_{exp}) were 0.102, 0.105, and 0.107 mmol/g for the Cd initial concentrations of 1.0, 1.5, and 2.0 mmol/L. The equilibrium was reached in 45 min, with removal percentage values of 81, 75, and 58%, in this order. The sodium modification implied changes in the adsorptive kinetic behavior. Figure 8 (b) shows that faster kinetics were found for VNa, with equilibrium time of 10 min, removal percentages of 99.4, 99.9, and 99.2%, and q_{exp} of 0.130, 0.177, and 0.276 mmol/g for the initial concentrations of 1.0, 1.5, and 2.0 mmol/L, respectively. The experimental values (q_{exp}) demonstrate that the cation displacement by sodium on the modified adsorbent surface made the surface more homogenous, facilitating the ion exchange between sodium and cadmium, and improving process efficiency. The surface charge analysis, Fig. 4, had already indicated a possible favoring of adsorption on VNa due to electrostatic forces, since the surface charges became more negative after sodification. Almeida Neto et al. (2014) also observed that the clay treatment with sodium improved the adsorptive properties in the nickel and copper ion removal, since there was an increase of exchangeable Na$^+$ in the Bofe bentonite surface. Lima et al. (2019) achieved better adsorptive capacities for Ca^{2+} removal with sodium-modified vermiculite, compared with raw vermiculite. The authors applied a different sodification process from the one applied in the present work, sodifying the raw vermiculite only in saline solution, and the water softening process was performed at pH 10. At this pH, the OH$^-$ activity increases neutralizing acidic groups which results in the cation adsorption by saturation (Mathialagan and Viraraghavan 2003).

Table 4 shows the fit parameters of the PFO, PSO, resistance to mass transfer in the external film (RMT), intraparticle diffusion (ID), and Boyd's kinetic models for the adsorption kinetics with initial Cd^{2+} concentration of 1.0, 1.5, and 2.0 mmol/L in EV and VNa clays, and Fig. 9 presents the adjustments of the models to the experimental data.

From Figs. 8 and 9 and Table 4, it can be seen that higher values of adsorbed quantity (q_{exp}) were obtained for the VNa clay. In percentage terms, there were increases of 27.5%,

68.6%, and 157.9% when the initial concentrations of Cd^{2+} were 1.0 mmol/L, 1.5 mmol/L, and 2 mmol/L, respectively. These increases are strictly associated with the modification process to which the clay was subjected. The sodification process in the acid medium was able to displace several ions from the solid structure that Cd^{2+} alone was not able to. In the latter case, the lower q_{exp} by EV clay reflects this difficulty.

From Table 4 and Fig. 9, it is observed that the PSO model presented the best fit to the experimental data compared to the PFO. Higher R^2 and lower RMD and AICc values were obtained by the PSO model. The PSO model assumes that the adsorption rate is related to the quantity of active sites available on the solid surface (Kajjumba et al. 2019) and that chemical adsorption is responsible for adsorption by means of sharing electrons (Gu et al. 2019). The best fit for PSO is consistent with the ion exchange process that is related to the structure and surface characteristics of the EV and VNa clays, since this process involves the displacement of ions from the solid by the adsorbate in the same site. In fact, ion exchange is the most significant process in the cadmium adsorption in EV and VNa. Comparing the PSO adjustments for EV and VNa results, better fits are observed for the modified VNa clay, since in this clay the ion exchange is facilitated by the major displacement of a single type of ion (Na$^+$). Better fits for the PSO model were observed by Chen et al. (2018) in Cd^{2+}adsorption by raw vermiculite and its biocomposite with chitosan with an equilibrium time of 30 min for both adsorbents. Better fits for the PSO model in toxic metal adsorption kinetics were observed by Mathialagan and Viraraghavan (2003) with raw vermiculite, Chen et al. (2018) with raw vermiculite and its biocomposite with chitosan, Gu et al. (2018) with amine-functionalized vermiculite, and Gu et al. (2019) with g-polyacrylamide/vermiculite indicating that for vermiculite and its modifications, such as the sodification process applied in the present work, the PSO model is the one that best describes the kinetics data.

The RMT model showed a very similar fit to the PFO, presenting very close RMD and AICc values. The R^2 indicates a good fit of the model to the experimental data, with values close to 1, mainly for the system with VNa. The k_{MT} value is higher for the system with VNa, which indicates that the mass transfer resistance in external film influences the kinetic speed in this system more than in the system with EV. The EV's greater complexity composition is related to what was observed. In the adsorptive process in the EV system, after overcoming the mass transfer resistance in an external film, the solute will still undergo stages of ion displacement and rearrangement on the solid surface, as there is ion exchange and possible ion rearrangement, such as K$^+$ and Mg^{2+} that is part of the EV adsorbent constitution. In the system with VNa, after the transfer in the film,
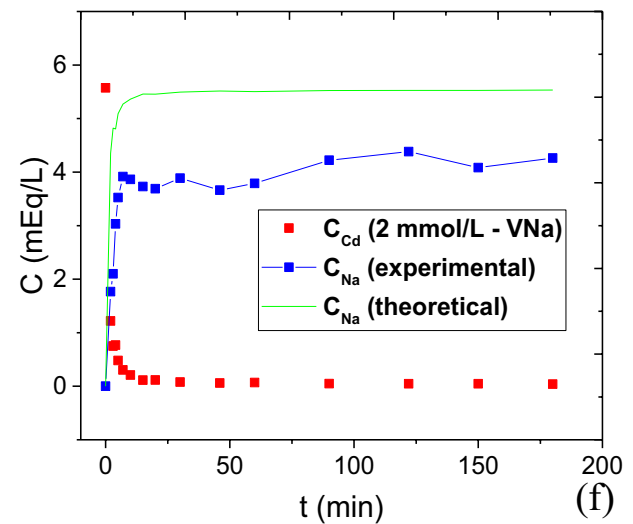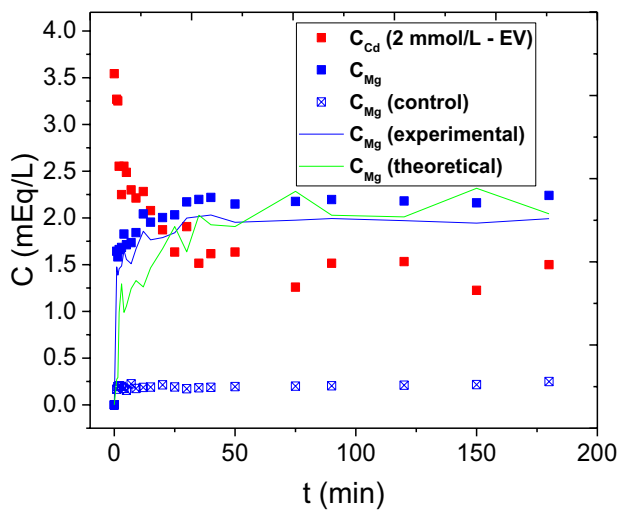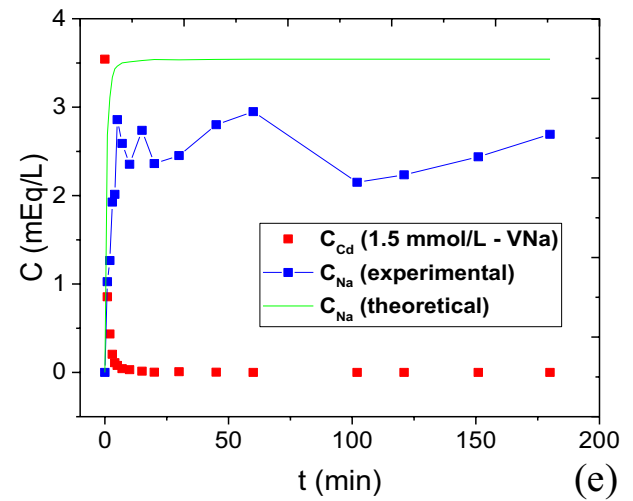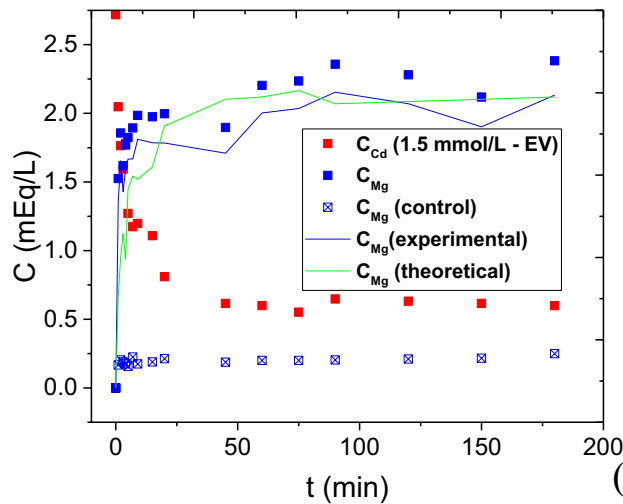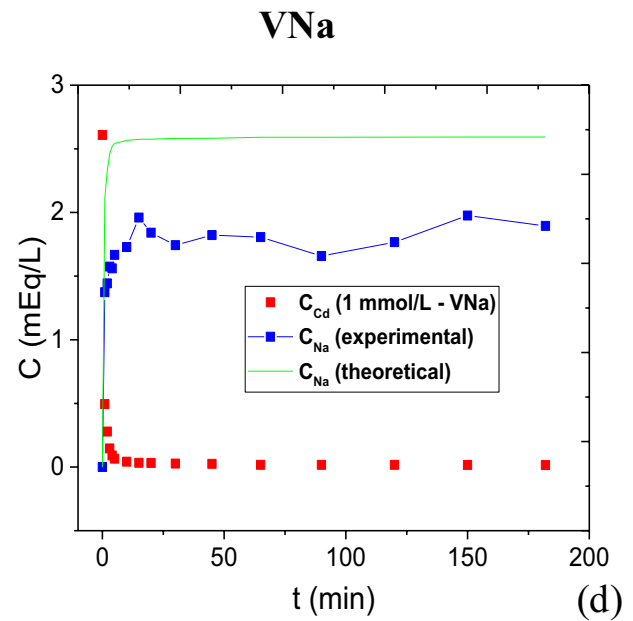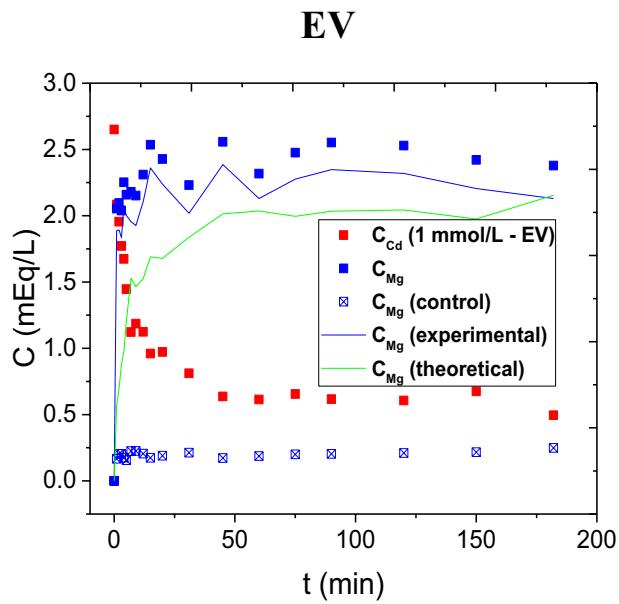
EV

VNa

◄**Fig. 7** Experimental and theoretical profiles of the exchangeable ion release for the adsorbent-initial concentration systems: (a) EV – 1 mmol/L; (b) EV – 1.5 mmol/L; (c) EV – 2 mmol/L; (d) VNa – 1 mmol/L; (e) VNa – 1.5 mmol/L; (f) VNa – 2 mmol/L

ion exchange occurs in a simpler way and the adsorptive attachment occurs very quickly (Tran et al. 2017). This is reflected in the faster kinetics observed in the system with VNa. The decrease in k_{MT} values with the increase of the initial concentration in the system with VNa occurs due to the solute greater availability in liquid phase, which increases the driving force (mass transfer gradient), resulting in less time in this step.

In the fits of the ID model, plots of q versus $t^{0.5}$ indicated three linear regions: in the first, instantaneous adsorption (external surface adsorption) occurs; in the second, intrapartic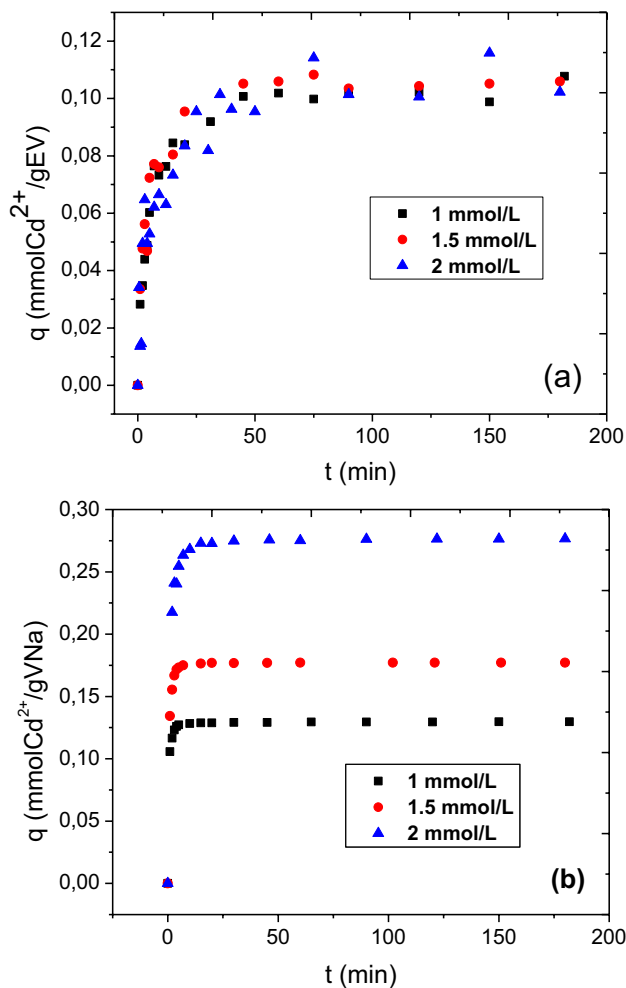le diffusion is the controlling step; and the third represents the equilibrium region (Wu et al. 2009). Multilinearity indicates that the three stages are involved in the cadmium adsorptive process in EV and VNa. The second step linear adjustment was obtained, which indicates that the intraparticle diffusion must contribute to the mass transfer mechanism. However, due to the fact that plots did not pass through the origin, intraparticle diffusion cannot be considered the process limiting step. In this case, it is confirmed that the mass transfer resistance in external film may be the step that governs the Cd^{2+} adsorption. This step was also lower for sodified vermiculite, revealing that the adsorbent treatment with sodium favored the mass transfer mechanisms.

Boyd's model fit to the data confirmed that external diffusion controls the rate of cadmium adsorption on EV and VNa clays. The linear function resulted in a satisfactory R^2 and low RMD (%) values and the plot did not pass the origin, which indicates that the adsorption process is limited by diffusion in the boundary layer on the adsorbent surface (Silva et al. 2021; Kajjumba et al. 2019), according to previous analysis of other evaluated models.

In short, the kinetics results demonstrated that the sodification process is important to improve the adsorbent properties, i.e., to obtain a higher adsorptive capacity in the clay and a faster kinetics of only 10 min. The adsorption controlling step is the resistance to mass transfer on external film with adsorptive attachment by chemisorption, related to ion exchange. The results indicate that the clay has the potential to be employed for cadmium removal from an aqueous solution.

Fig. 8 Cd^{2+} adsorption kinetics in (a) expanded vermiculite (EV), and (b) sodified vermiculite (VNa)

Conclusions

The present study shows that expanded vermiculite and its modification with sodium in an acid medium have great potential for Cd^{2+} removal from an aqueous solution. The sodification process is simple and was performed in a low-cost commercial clay, producing a material with higher adsorptive capacity with faster adsorption kinetics, compared to its initial form.

For both systems evaluated, the PSO model best described the experimental data, indicating that chemisorption is involved in the adsorptive process, which is consistent with the observed ion exchange. The ID, RMT, and Boyd models' fit showed that mass transfer resistance in external film may be the step that governs

Table 4 Parameters obtained from adsorption kinetic model adjustment for the cadmium single-component adsorption in EV and VNa clays

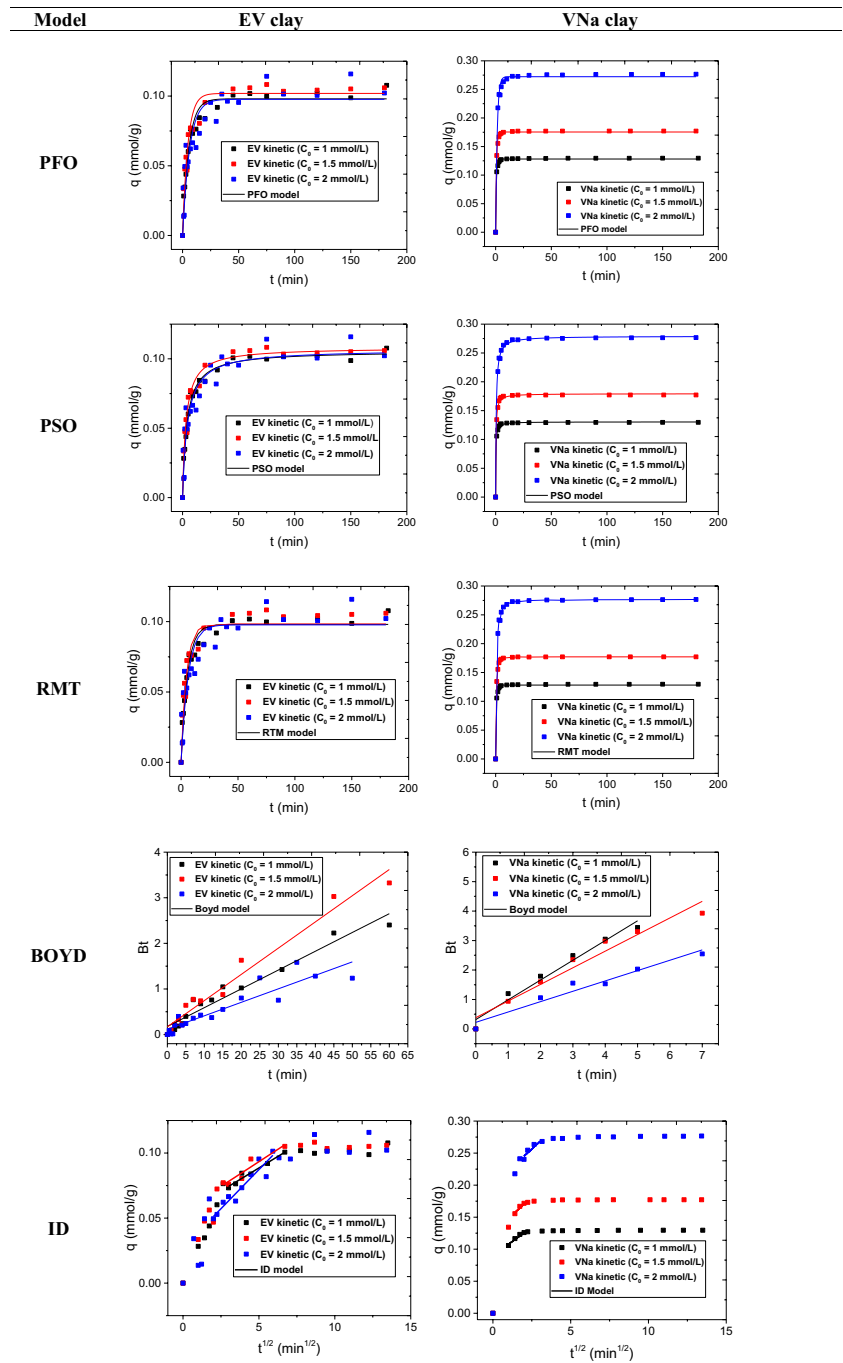| Model	Parameters	EV			VNa		
		1.0 mmol/L	1.5 mmol/L	2.0 mmol/L	1.0 mmol/L	1.5 mmol/L	2.0 mmol/L
Experimental	q_{exp} (mmol/g)	0.102	0.105	0.107	0.130	0.177	0.276
PFO	q_e (mmo/g)	0.098	0.102	0.098	0.128	0.175	0.272
	k_1 (min^{-1})	0.179	0.214	0.159	1.611	1.326	0.713
	R^2	0.957	0.930	0.843	0.994	0.994	0.991
	RMD (%)	8.130	10.657	16.248	1.407	1.442	1.865
	AICc	−183.6	−153.7	−191.2	−183.9	−175.1	−152.0
PSO	q_e (mmol/g)	0.106	0.108	0.107	0.130	0.179	0.279
	k_2 (g/(mmol.min))	2.437	2.996	2.110	35.028	19.012	6.781
	R^2	0.986	0.970	0.901	0.999	0.997	0.998
	RMD (%)	7.096	6.522	10.225	0.645	1.110	0.819
	AICc	−204.8	−168.3	−214.4	−209.4	−184.9	−179.2
RMT	k_{MT} (min^{-1})	0.013	0.015	0.088	1.583	1.311	0.697
	R^2	0.980	0.928	0.929	0.997	0.997	0.995
	RMD (%)	8.130	10.652	16.250	1.407	1.423	1.864
	AICc	−186.5	−154.3	−193.9	−187.0	−179.0	−155.1
Boyd	D_i (cm^2/s)	1.27 0.10^{-7}	1.77 0.10^{-7}	9.12 0.10^{-8}	2.07 0.10^{-6}	1.74 0.10^{-6}	1.08 0.10^{-6}
	R^2	0.950	0.968	0.846	0.970	0.955	0.954
	RMD (%)	0.416	0.230	1.305	0.065	0.061	0.074
ID	K_d (mmol/(g.min$^{1/2}$))	0.0071	0.0076	0.01202	0.0175	0.02171	0.02225
	C (mmol/g)	0.0531	0.0554	0.0272	0.0901	0.1267	0.20073
	R^2	0.951	0.869	0.890	0.921	0.867	0.782

the Cd^{2+} adsorption. Removals greater than 99% were achieved in the kinetics with the VNa clay, and the adsorptive capacity reached 0.107 and 0.276 mmol/g for the EV and VNa clays, respectively, under the evaluated conditions. The VNa clay had a higher adsorption rate reaching equilibrium in 10 min, while the EV clay took 45 min.

The CEC was 210.44 mEq/100 g for EV and 233.19 mEq/100 g for VNa. In addition, it was shown that only the exchangeable ions Mg^{2+} and Na$^+$ are relevant in the ion exchange. In ion exchange kinetics, the expanded vermiculite showed a behavior close to the stoichiometric of 1:1 between Mg^{2+} and Cd^{2+}, respecting the principle of electroneutrality. On the other hand, the sodified vermiculite absorbed about 72% of the sodium expected theoretically, due to the treatment with sodium at acidic pH. The FTIR spectra did not indicate pronounced variations in the functional groups of the structure adsorbent. Only slight variations were observed in the exchange groups of metals bonded to oxygen and silicon. The XRD diffractograms indicated a decrease in the distance between the layers after the modification and adsorption processes, due to the interaction with water and exchangeable ions.

The clay EV has its isoelectric point at pH 2.5 and clay VNa has a negative charge over the entire pH range evaluated. From the analysis of the metallic speciation diagrams as a function of pH and determination of pH$_{ZPC}$, pH 6 was chosen to carry out the adsorption experiments. At pH 6 the surface charges favor Cd^{2+} adsorption by electrostatic forces. The micrographs showed that there was a space contraction between the clay layers after the sodium treatment and Cd^{2+} adsorption processes, which promoted a decrease in the surface area. However, the VNa performance was superior compared to the EV.

Fig. 9 PFO, PSO, RTM, Boyd, and ID model fits to experimental data of Cd^{2+} adsorption on EV and VNa clays

Availability of data and material Not applicable.

Code availability Not applicable.

Declarations

Ethics approval and consent to participate Not applicable.

Consent for publication Not applicable.

Competing interests The authors declare no competing interests.

References

Alexander JA, Surajudeen A, Aliyu E-IU, Omeiza AU, Zaini MAA (2017) Multi-metals column adsorption of lead(II), cadmium(II) and manganese(II) onto natural bentonite clay. Water Sci Technol 76(8):2232–2241. https://doi.org/10.2166/wst.2017.391

Almeida Neto AF, Vieira MGA, Silva MGC (2014) Insight of the removal of nickel and copper ions in fixed bed through acid activation and treatment with sodium of clay. Braz J Chem Eng 31(4):1047–1056. https://doi.org/10.1590/0104-6632.20140314s00001976

Anjos VE, Rohwedder JR, Cadore S, Abate G, Grassi MT (2014) Montmorillonite and vermiculite as solid phases for the preconcentration of trace elements in natural waters: adsorption and desorption studies of As, Ba, Cu, Cd, Co, Cr, Mn, Ni, Pb, Sr, V, and Zn. Appl Clay Sci 99:289–296. https://doi.org/10.1021/acs.iecr.9b00045

Bonate PL (2011) Pharmacokinetic-pharmacodynamic modeling and simulation, 2nd edn. Springer, New York

Borba CE, Silva EA, Spohr S, Santos GHF, Guirardello R (2010) Ion exchange equilibrium prediction for the system $Cu^{2+}-Zn^{2+}-Na^+$. J Chem Eng Data 55:1333–1341. https://doi.org/10.1021/je900649e

Boyd GE, Adamson AW, Myers LS (1947) The exchange adsorption of ions from aqueous solutions by organic zeolites. J Am Chem Soc 69(11):2836–2848. https://doi.org/10.1021/ja01203a066

Brião GV, Silva MGC, Vieira MGA (2020) Neodymium recovery from aqueous solution through adsorption/desorption onto expanded vermiculite. Appl Clay Sci 198:105825. https://doi.org/10.1016/j.clay.2020.105825

Cantuaria ML, Almeida Neto AF, Nascimento ES, Santos OAA, Vieira MGA (2014) Removal of Silver Ions on Calcined Verde-lodo Bentonite Clay: Equilibrium Study. Chem Eng Trans 39:667–672. https://doi.org/10.3303/CET1439112

Cantuaria ML, Nascimento ES, Almeida Neto AF, Dos Santos OAA, Vieira MGA (2015) Removal and recovery of silver by dynamic adsorption on bentonite clay using a fixed-bed column system. Adsorpt Sci Technol 33(2):91–103. https://doi.org/10.1260/0263-6174.33.2.91

Cantuaria ML, Almeida Neto AF, Nascimento ES, Vieira MGA (2016) Adsorption of silver from aqueous solution onto pre-treated bentonite clay: complete batch system evaluation. J Clean Prod 112:1112–1121. https://doi.org/10.1016/j.jclepro.2015.07.021

Chen L, Wu P, Chen M, Lai X, Ahmed Z, Zhu N, Zhi D, Bi Y, Liu T (2018) Preparation and characterization of the eco-friendly chitosan/vermiculite biocomposite with excellent removal capacity for cadmium and lead. Appl Clay Sci 159:4–82. https://doi.org/10.1016/j.clay.2017.12.050

Chowdhury R, Ramond A, O'Keeffe LM, Shahzad S, Kunutsor SK, Muka T, Gregson J, Willeit P, Warnakula S, Khan H, Chowdhury S, Gobin R, Franco OH, Angelantonio E (2018) Environmental toxic metal contaminants and risk of cardiovascular disease: systematic review and meta-analysis. BMJ 362:k3310. https://doi.org/10.1136/bmj.k3310

Freitas ED, Almeida HJ, Vieira MGA (2017a) Binary adsorption of zinc and copper on expanded vermiculite using a fixed bed column. Appl Clay Sci 146:503–509. https://doi.org/10.1016/j.clay.2017.07.004

Freitas ED, Carmo ACR, Almeida Neto AF, Vieira MGA (2017b) Binary adsorption of silver and copper on Verde-lodo bentonite: kinetic and equilibrium study. Appl Clay Sci 137:69–76. https://doi.org/10.1016/j.clay.2016.12.016

Gañán-Gómez J, Macías-García A, Díaz-Díez MA, González-García C, Sabio-Rey E (2006) Preparation and characterization of activated carbons from impregnation pitch by ZnCl. Appl Surf Sci 252(17):5976–5979. https://doi.org/10.1016/j.apsusc.2005.11.011

Gu S, Wang L, Mao X, Yang L, Wang C (2018) Selective adsorption of Pb(II) from aqueous solution by triethylenetetramine-grafted polyacrylamide/vermiculite. Materials 11(4):514. https://doi.org/10.3390/ma11040514

Gu S, Kang X, Wang L, Lichtfouse E, Wang C (2019) Clay mineral adsorbents for heavy metal removal from wastewater: a review. Environ Chem Lett 17:629–654. https://doi.org/10.1007/s10311-018-0813-9

Ho YS, Mckay G (1998) A comparison of chemisorption kinetic models applied to pollutant removal on various sorbents. Process Saf Environ Prot 76(B):332–340. https://doi.org/10.1205/095758298529696

Howard BH, Lekse JW (2018) Clay Mineralogy. In: Romanov V. (eds) Greenhouse gases and clay minerals. Cham: Springer, 55–75. https://doi.org/10.1007/978-3-319-12661-6_4

Kajjumba GW, Emi S, Öngen A, Özcan HK, Aydin S (2019) Modelling of adsorption kinetic processes - errors, theory and application, in Edebali S (Eds.), Advanced Sorption Process Applications, Intechopen, 1–19. https://doi.org/10.5772/intechopen.80495

Lagergren S (1898) Zur theorie der sogenannten adsorption gelöster stoffe, KungligaSvenska Vetenskapsakademiens – Translate to English: "About the theory of so-called adsorption of soluble substances, Kungliga Svenska Vetenskapsakademien." Handlingar 24:1–39

Lima LF, Andrade JR, Silva MGC, Vieira MGA (2017) Fixed bed adsorption of benzene, toluene, and xylene (BTX) contaminants from monocomponent and multicomponent solutions using a commercial organoclay. Ind Eng Chem Res 56(21):6326–6336. https://doi.org/10.1021/acs.iecr.7b00173

Lima RRC, Lima PDS, Greati VR, Sousa PBF, Medeiros GVS (2019) Sodium-modified vermiculite for calcium ion removal from aqueous solution. Ind Eng Chem Res 58:9380–9389. https://doi.org/10.1021/acs.iecr.9b00045

Liu S, Wu P, Yu L, Li L, Gong B, Zhu N, Dang Z, Yang C (2017) Preparation and characterization of organo-vermiculite based on phosphatidylcholine and adsorption of two typical antibiotics. Appl Clay Sci 137:160–167. https://doi.org/10.1016/j.clay.2016.12.002

Madejová J (2003) FTIR techniques in clay mineral studies review. Vib Spectrosc 31:1–10. https://doi.org/10.1016/S0924-2031(02)00065-6

Malandrino M, Abollino O, Giacomino A, Aceto M, Mentasti E (2006) Adsorption of heavy metals on vermiculite: influence of pH and organic ligands. J Colloid Interface Sci 299:537–546. https://doi.org/10.1016/j.jcis.2006.03.011

Marcos C, Rodríguez I (2014) Exfoliation of vermiculites with chemical treatment using hydrogen peroxide and thermal treatment using microwaves. Appl Clay Sci 87:219–227. https://doi.org/10.1016/j.clay.2013.11.008

Mathialagan T, Viraraghavan T (2003) Adsorption of cadmium from aqueous solutions by vermiculite. Sep Sci Technol 38(1):57–76. https://doi.org/10.1081/SS-120016698

Moraes DS, Rodrigues EMS, Lamarão CN, Marques GT, Rente AFS (2019) New sodium activated vermiculite process. Testing on Cu2+ removal from tailing dam waters. J Hazard Mater 366:34–38. https://doi.org/10.1016/j.jhazmat.2018.11.086

Nishikawa E, Almeida Neto AF, Vieira MGA (2012) Equilibrium and thermodynamic studies of zinc adsorption on expanded vermiculite. Adsorpt Sci Technol 30(8–9):759–772. https://doi.org/10.1260/0263-6174.30.8-9.759

Oliveira MF, Silva MGC, Vieira MGA (2019) Equilibrium and kinetic studies of caffeine adsorption from aqueous solutions on thermally modified Verde-lodo bentonite. Appl Clay Sci 168:366–373. https://doi.org/10.1016/j.clay.2018.12.011

Pérez-Maqueda LA, Balek V, Poyato J, Pérez-Rodríquez JL, Šubrt J, Bountsewa IM, Beckman IN, Málek Z (2003) Study of natural and ion exchanged vermiculite by emanation thermal analysis, TG, DTA and XRD. J Therm Anal Calorim 71(3):715–726

Potter MJ (2010) Vermiculite, U.S. Geological Survey Minerals Yearbook – 2007, USGS. https://s3-us-west-2.amazonaws.com/prd-wret/assets/palladium/production/mineral-pubs/vermiculite/myb1-2007-vermi.pdf (accessed 28 Feb 2021)

Puigdomenech I (2010) Chemical equilibrium diagrams. Hydra/Medusa; Sweden: Inorganic Chemistry Royal Institute of Technology (KTH)

Puranik PR, Modak JM, Paknikar KMA (1999) A comparative study of the mass transfer kinetics of metal biosorption by microbial biomass. Hydrometallurgy 52:189–197. https://doi.org/10.1016/S0304-386X(99)00017-1

Russell JD, Fraser AR (1994) Infrared methods. In: Wilson MJ (Ed.), Clay Mineralogy: Spectroscopic and Chemical Determinative Methods. London: Chapman & Hall. https://doi.org/10.1007/978-94-011-0727-3

Ryabchenko KV, Yanovska ES, Tertykh VA, Kichkiruk OYu, Sternik D (2014) Adsorption properties of vermiculite with in situ–immobilized polyaniline with respect to Cr(VI), Mo(VI), W(VI), V(V) and P(V) anions. Adsorp Sci Technol 32(1):89–99. https://doi.org/10.1260/0263-6174.32.1.89

Sarkar B, Rusmin R, Ugochukwu UC, Mukhopadhyay R. Manjaiah KM (2019) Chapter 5 - Modified clay minerals for environmental application, in Modified Clay and Zeolite Nanocomposite Materials, Elsevier Inc. https://doi.org/10.1016/B978-0-12-814617-0.00003-7

Silva TL, Silva Junior AC, Vieira MGA, Silva MGC (2016) Biosorption study of copper and zinc by particles produced from silk sericin - alginate blend: evaluation of blend proportion and thermal cross-linking process in particles production. J Clean Prod 137:1470–1478. https://doi.org/10.1016/j.jclepro.2015.05.067

Silva TL, Silva MGC, Vieira MGA (2021) Palladium adsorption on natural polymeric sericin-alginate particles crosslinked by polyethylene glycol diglycidyl ether. J Environ Chem Eng 9:105617. https://doi.org/10.1016/j.jece.2021.105617

Sis H, Uysal T (2014) Removal of heavy metal ions from aqueous medium using Kuluncak (Malatya) vermiculites and effect of precipitation on removal. Appl Clay Sci 95:1–8. https://doi.org/10.1016/j.clay.2014.03.018

Stawinski W, Wegrzyn A, Danko T, Freitas O, Figueiredo S, Chmielarz L (2017) Acid-base treated vermiculite as high performance adsorbent: insights into the mechanism of cationic dyes adsorption, regeneration, recyclability and stability studies. Chemosphere 173:107–115. https://doi.org/10.1016/j.chemosphere.2017.01.039

Thommes M, Kaneko K, Neimark AV, Olivier JP, Rodriguez-Reinoso F, Rouquerol J, Sing KSW (2015) Physisorption of gases, with special reference to the evaluation of surface area and pore size distribution (IUPAC technical report). Pure Appl Chem 87. https://doi.org/10.1515/pac-2014-1117

Tran HN, You SJ, Bandegharaei AH, Chao HP (2017) Mistakes and inconsistencies regarding adsorption of contaminants from aqueous solutions: a critical review. Water Res 120:88–116. https://doi.org/10.1016/j.watres.2017.04.014

US Geological Survey, Mineral Commodity Summaries (2021) https://pubs.usgs.gov/periodicals/mcs2021/mcs2021-vermiculite.pdf (accessed 28 Feb 2021)

Vardhan KH, Kumar PS, Panda RC (2019) A review on heavy metal pollution, toxicity and remedial measures: current trends and future perspectives. J Mol Liq 290:111197. https://doi.org/10.1016/j.molliq.2019.111197

Volesky B, Yeoung-Sang Y, Park D, Park JM (2001) Biosorption of trivalent chromium on the brow seaweed biomass. Environ Sci Technol 35:3543–4358. https://doi.org/10.1021/es010866k

Weber WJ, Morris JC (1963) Kinetics of adsorption on carbon from solution. J Sanit Eng Div 89(2):31–60

Wu FC, Tseng RL, Juang RS (2009) Initial behavior of intraparticle diffusion model used in the description of adsorption kinetics. Chem Eng J 153:1–8. https://doi.org/10.1016/j.cej.2009.04.042